Degenerative Lumbar Spine Disease: Imaging and Biomechanics

Maxime Lacroix, MD[1,2] Christelle Nguyen, MD, PhD[3] Robert Burns, MD[1] Amandine Laporte, MD[1] François Rannou, MD, PhD[3] Antoine Feydy, MD, PhD[1]

[1] Department of Musculoskeletal Radiology, Hôpital Cochin, Université de Paris, Paris, France
[2] Department of Radiology, Hôpital Européen Georges-Pompidou, Université de Paris, Paris, France
[3] Department of Physical and Rehabilitation Medicine, Hôpital Cochin, Université de Paris, Paris, France

Address for correspondence Antoine Feydy, MD, PhD, Service de Radiologie B, Hôpital Cochin – APHP, Université de Paris, 27 rue du Faubourg Saint-Jacques, 75679 Paris CEDEX 14, France (e-mail: antoine.feydy@aphp.fr).

Semin Musculoskelet Radiol 2022;26:424–438.

Abstract

Chronic low back pain (CLBP) is one of the most common diagnoses encountered when considering years lived with disability. The degenerative changes of the lumbar spine include a wide spectrum of morphological modifications visible on imaging, some of them often asymptomatic or not consistent with symptoms. Phenotyping by considering both clinical and imaging biomarkers can improve the management of CLBP. Depending on the clinical presentation, imaging helps determine the most likely anatomical nociceptive source, thereby enhancing the therapeutic approach by targeting a specific lesion. Three pathologic conditions with an approach based on our experience can be described: (1) pure painful syndromes related to single nociceptive sources (e.g., disk pain, active disk pain, and facet joint osteoarthritis pain), (2) multifactorial painful syndromes, representing a combination of several nociceptive sources (such as lumbar spinal stenosis pain, foraminal stenosis pain, and instability pain), and (3) nonspecific CLBP, often explained by postural (muscular) syndromes.

Keywords
- spine
- diagnostic Imaging
- magnetic resonance imaging
- pain
- low back pain

Chronic low back pain (CLBP) is one of the most common diagnoses when considering years lived with disability.[1] An estimated 5 to 10% of individuals experience back pain in their lifetime.[2]

The spine is a compromise between stability and mobility. From a biomechanical point of view, it is a multiarticular structure composed of numerous segments, enabling multidirectional movement and the management of large complex loads. Two adjacent vertebrae, the intervertebral disk, several spinal ligaments, and facet joints between them constitute a functional spinal unit.[3] During life, the spine undergoes continuous changes as a response to physiologic axial load.[4] These degenerative changes include a wide spectrum of morphological modifications visible on imaging, some of them often asymptomatic and not consistent with symptoms.

CLBP has tended to be demedicalized for several years.[5] However, phenotyping CLBP by taking into account both clinical and imaging biomarkers can improve patient management. Depending on the clinical presentation, imaging helps determine the most likely anatomical nociceptive source, thereby enhancing the therapeutic approach by targeting a specific lesion.

This article focuses on three pathologic conditions with an imaging approach based on our clinical experience and research[6]:

- Pure painful syndromes: Single nociceptive sources including disk pain, active disk pain, and facet joint osteoarthritis pain
- Multifactorial painful syndromes: A combination of several nociceptive sources, such as lumbar spinal

Issue Theme Spine Imaging; Guest Editors, Alberto Bazzocchi, MD, PhD and Giuseppe Guglielmi, MD

Thieme Medical Publishers, Inc., 333 Seventh Avenue, 18th Floor, New York, NY 10001, USA

DOI https://doi.org/10.1055/s-0042-1748912.
ISSN 1089-7860.

stenosis pain, foraminal stenosis pain, and instability pain
- Nonspecific lower back pain: Often explained by postural (muscular) syndromes

Pure Painful Syndromes

Based on our experience and practice-based approach, we consider pure painful syndromes to be related to single nociceptive sources. We include in this category disk pain, active disk pain, and facet joint osteoarthritis pain.

Disk Pain

Definition, Anatomy, and Biomechanics

Degenerative disk disease (DDD) usually affects middle-aged adults (< 55 years of age), and the disk is the anatomical entity responsible. A dull and aching pain characterizes the syndrome. Prolonged sitting, spinal extension movements, and a spinal hyperextension position generally intensify the pain.

The intervertebral disk is a complex multicomponent avascular structure consisting of an outer fibrous ring (annulus fibrosus) and an inner hydrated gel-like substance (nucleus pulposus).[7] The nucleus pulposus is more hydrated than the annulus fibrosus (because of its high concentration in proteoglycans).[7] Due to the contrast of this double fibrous and hydrated component, magnetic resonance imaging (MRI) is the best examination to analyze the intervertebral disk, particularly on T2-weighted (T2w) sequences. On MRI, the nucleus pulposus and the inner zone of the annulus fibrosus are not distinguishable and appear as high signal on T2w images (►**Fig. 1a**). The outer zone of the annulus fibrosus (Sharpey's fibers) appears as a low signal on T2w images (►**Fig. 1a**). The intervertebral disk is avascular. Its nutrition is provided by diffusion through the cartilaginous end plates that connect the intervertebral disk with the adjacent vertebral bodies. This explains why the disk is not enhanced after injection of gadolinium chelate.

DDD is an incompletely understood multifactorial process characterized by physical, biochemical, and histologic changes of the disk and the cartilaginous end plates, with probable genetic predisposition, generally starting after age 30 years.[8] It is most frequent at the lower lumbar levels, particularly at L5–S1.[9] These changes modify the ability of the disk to sustain and transmit forces.

Imaging

The terminology used for disk abnormalities includes many labels that vary depending on the clinical team's preferences. On imaging, we can schematically differentiate:

- Reduction in signal intensity of the disk (particularly on T2w sequences)
- Disk height loss
- Disk fissures (in particular, annular fissures)
- Disk bulging with and without remodeling of end plates
- Disk protrusion/Extrusion

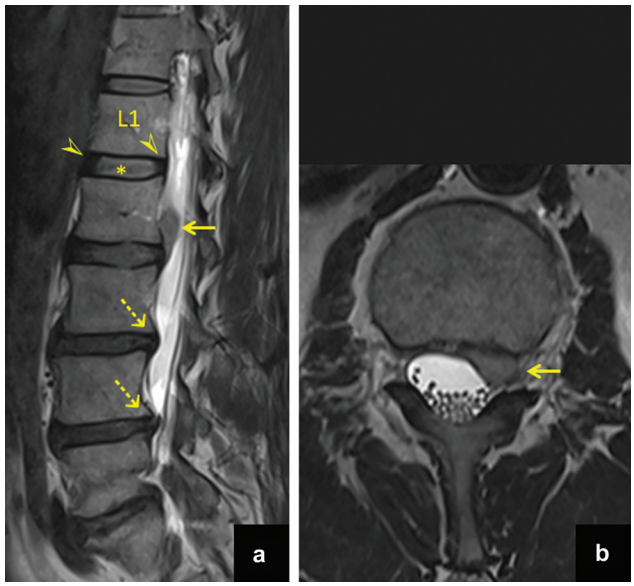

Fig. 1 A 35-year-old patient with left radiculalgia. (**a**) Sagittal T2-weighted (T2w) image. (**b**) Axial T2w image at the L2–L3 level. The L1–L2 disk is normal: The nucleus pulposus and the inner zone of the annulus fibrosus are not distinguishable and appear as high signal on T2w images (asterisk), whereas the outer zone of the annulus fibrosus (Sharpey distinguishable) appears as low signal on the T2w images (arrowhead). At the L2–L3 level: left posterolateral L2–L3 disk extrusion with superior migration (arrows). At the L3–L4 and L4–L5 levels: disk bulging corresponding to a posterior displacement of disk material beyond the margins of the intervertebral space (dashed arrows) with disk height loss and global low signal of the corresponding disks due to degenerative changes.

- Intravertebral disk herniation (included or not in Scheuermann's disease)

Reduction in signal intensity of the disk, disk height loss, disk bulging, and remodeling of the end plates are documented in almost 90% of asymptomatic patients > 60 years of age.[10] The responsibility for these morphological modifications and CLBP are frequently controversial.[11,12] This suggests that such changes, especially those discovered incidentally, can be considered as a natural part of the aging process and do not require therapeutic intervention.

However, disk protrusion/extrusion and disk fissures do not show a significant increase in incidence with increased age, possibly suggesting they are not part of the natural aging process.[10] Nevertheless, these two lesions may also be seen in asymptomatic patients, which should lead to caution in establishing a causal relationship with pain.

The prevalence of degenerative features may also vary between different populations. For instance, a study found DDD was present in ~ 80% and disk herniation in ~ 30% of asymptomatic high-level athletes with a mean age of 18 years.[13]

Technically, according to some authors, a sagittal T2w Dixon sequence may be sufficient to detect common degenerative changes of the lumbar spine accurately in patients with CLBP.[14,15] Depending on diagnostic needs, further sequences (e.g., axial T2w sequences at the levels of suspected pathology) can be performed.[15]

Reduction in Signal Intensity and Disk Height Loss

The first stage of DDD is a progressive dehydration (in particular of the nucleus pulposus) and the concomitant increase of relative collagen content. This is responsible for collapsing of the disk. Thus DDD is also often associated with a decrease in disk height (►**Fig. 1a**).

On radiographs, the disk is not directly visible: DDD appears as a narrowing of the intervertebral space. On computed tomography (CT), the detailed analysis of the disk is also limited to an analysis of calcifications, intradiskal gas, and the narrowing of the intervertebral space.

On MRI, degenerative disk modifications are visible as a low signal, particularly on T2w images (►**Fig. 1a, b**). The volume and height of disks decrease with age, and their shape becomes less convex independently from degenerative modifications.[16] Pfirrmann initially graded degenerative changes on a five-grade classification.[17] This classification considers the structure of the disk, the ability to distinguish the nucleus pulposus and annulus fibrosus, and the signal intensity and height of the disk. However, there is no correlation between the Pfirrmann staging classification and clinical symptoms.[18]

Finally, advanced MR functional imaging techniques, such as T2 mapping, diffusion quantitative imaging, MR spectroscopy, and radionucleotide imaging, could provide measurements of some of the early degenerative changes.[7] For instance, quantitative MR techniques using T2 mapping of the disk can access the initial stages of DDD. The surveyed T2 values correlate with the water-storing capabilities of the nucleus pulposus and the collagen fiber density of the surrounding annulus fibrosus. Thus the nucleus pulposus T2 values decrease with disk degeneration while the T2 values increase in the annular regions.[19]

Disk Fissures

Degenerative changes are responsible for a reduction in vertebral bone elastic modulus and in changes in the mechanics of the intervertebral joints in flexion, extension, and torsion due to the desiccation of the nucleus pulposus.[20] The loss of function of the nucleus pulposus increases stress on the annulus fibrosus and can lead to the development of cracks and cavities, subsequently progressing to clefts and fissures. These annular fissures (AFs) are common, even in asymptomatic volunteers. Nevertheless, the defect due to AFs may allow ingrowth of granulation tissue, which explains why fissures near the dorsal root may be responsible for pain.

AFs are also an early sign of instability. They are not directly visible on imaging: Their detection is possible only if they are filled with a substance different from the disk (air or liquid). Two types of AFs are usually described (concentric and transverse).[21]

Concentric fissures correspond to "crescent" cavities located between two layers of the annulus fibrosus. They are secondary to a focal rupture of the transverse fibers that connect the layers of the annulus fibrosus to each other.[21] Transverse fissures correspond to irregular horizontal cavities located at the insertion of the peripheral fibers of the annulus fibrosus (Sharpey's fibers) on the anterior or posterior vertebral margin. In these two conditions, the intervertebral disk can be normal or degenerative. AF can lead to focal micro-abnormal mobility of the disk and, consequently, to traction phenomena on the fibers of the anterior longitudinal ligament that insert on the vertebral body at the level of Sharpey's fibers.

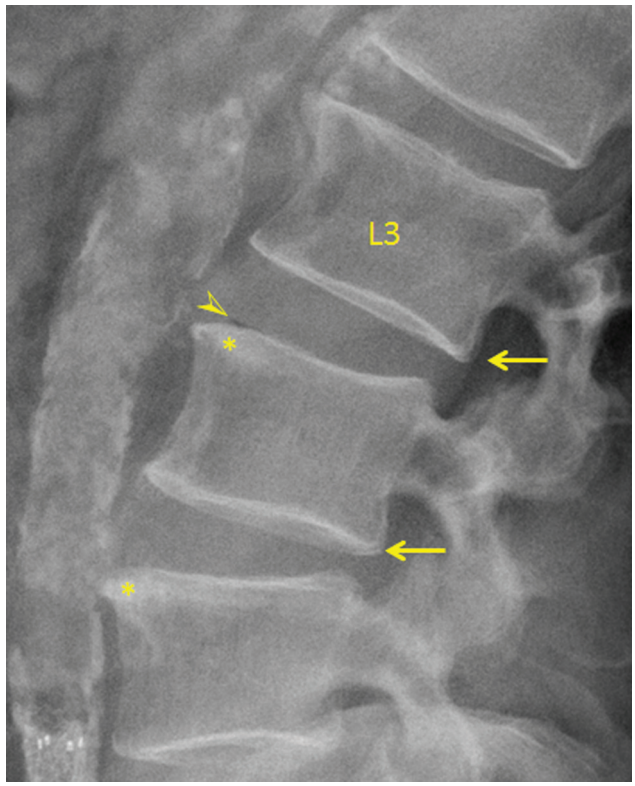

Fig. 2 Lateral radiograph centered at L3–L4 and L4–L5 levels in an 80-year-old patient. Annular fissure can be detected on radiographs if they contain gas and appears as a radiolucent horizontal cleavage, typically on an anterior vertebral margin, as in this case (arrowhead). Adjacent condensation of the anterior vertebral margins is related to vertebral body reactive changes (asterisks). Note degenerative retrolisthesis of L3 and L4 (arrows).

On radiographs or CT, AFs can be detected if they contain gas. They appear as a radiolucent horizontal cleavage, typically on an anterior vertebral margin (►**Fig. 2**). A "traction" enthesophyte developed in the fibers of the anterior longitudinal ligament, 2 to 3 mm under the projection of the vertebral endplate, is also an indirect sign of microinstability (Macnab's enthesophyte)[22] (►**Fig. 2**).

On MRI, AFs can be detected if they contain fluid: The term "high-intensity zone" (HIZ) is often used when the tear is situated in the posterior part of the annulus fibrosus. On MRI, HIZ corresponds to AF only if it appears as a high signal on T2w images (and as a low signal on T1w images). If there is a high signal on T1w images, it rather corresponds to calcified tissue (disk osteophytic protrusion)[23] (►**Fig. 3a, b**). The visibility of HIZ on several slices seems a reliable indicator for CLBP compared with patients with HIZ visible on only one slice.[24]

Slight edema of the anterior vertebral margin is sometimes visible (or sclerosis on radiographs/CT) and must not

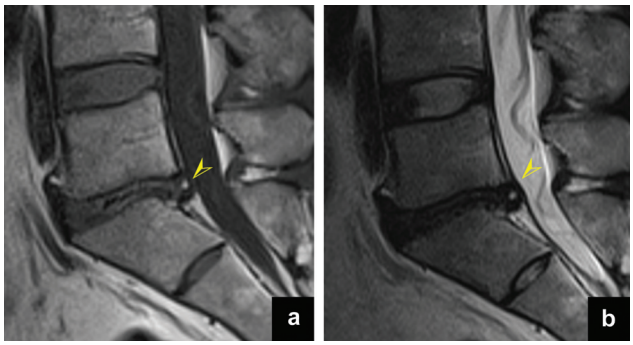

Fig. 3 A 40-year-old patient. (**a**) Sagittal T1-weighted magnetic resonance (MR) image. (**b**) Sagittal T2-weighted MR image: L5–S1 disk height decrease and retrolisthesis of L5 with posterior disk protrusion. Focal signal abnormality of the posterior part of the annulus fibrosus that appears in high signal on both sequences (arrowheads).

be interpreted as an inflammatory enthesitis fitting to a picture of spondyloarthritis.

Disk fissures can also be present in the nucleus pulposus. At the position changes, the intradiskal depression creates a cavity filled with air ("vacuum phenomenon").[25] Generally, after a few minutes, the fissure that initially contains air fills secondarily with fluid. When chronic, the content of these fissures can ossify, explaining the frequency of intradiskal calcifications on the imaging of the degenerative spine. They are characterized on radiographs or CT by opacities/high-density deposits, contrary to MRI where there is a considerable variability in signal intensity.[26]

Diskography consists of an intradiskal injection of an iodinated contrast medium (or gadolinium chelate in patients with a contraindication) under scopic or CT control. This technique is rarely used today. Nevertheless, when other examinations fail to localize the cause of pain, provocative diskography may occasionally be helpful if surgery is planned.[27] Although the injection itself may reproduce the patient's pain, the rate of false positives for intradiskal lesions primarily causing CLBP may reach 25%,[28,29] especially because low back pain seems to be strongly related to certain patient characteristics, such as their emotional profile.[30] When the disk is normal, the injection of contrast medium opacifies a well-limited central cavity, corresponding to the nucleus pulposus. In cases of disk degeneration, the contrast opacifies various AFs and even the epidural space.

Disk Bulging

Disk bulging is defined as a posterior displacement of disk material beyond the margins of the intervertebral space, with an extension < 3 mm beyond the edges of the vertebral body and along more than half of its circumferential length (> 180 degrees)[26] (►**Fig. 1a**). The prevalence of disk bulging is higher at L4–L5 and L5–S1, increases with age,[31] but it has no certain pathologic value because it is often seen in asymptomatic individuals.[3]

Disk Herniation

Disk herniation is a focal migration of the intervertebral disk material beyond the normal margins of the intervertebral disk space but involving less than half the circumference ($<$ 180 degrees), distinguishing it from disk bulging.[26] A disk herniation may include the nucleus pulposus, annular tissue, and/or vertebral end-plate debris. Disk herniation usually occurs in relatively young patients.[3]

Depending on their morphological appearance on imaging in the axial plane, disk herniations can be divided into two subtypes: disk protrusion and disk extrusion (with or without sequestration). In the axial plane, disk herniation can be classified as central, paracentral, foraminal, or extraforaminal. Generally, on CT or MRI, disk herniation has the same signal as the adjacent intervertebral disk, that is, low signal on T2w imaging. Nevertheless, when extruded, it may appear as high signal on T2w images. In any case, the disk herniation itself does not enhance after injection of contrast medium (only a rim enhancing surrounding the herniated disk is possible, probably explained by vascular granulation tissue).

Disk Protrusion

Disk protrusion corresponds to a focal or asymmetric extension of the disk beyond the intervertebral margins, with the base against the disk of origin broader than any other dimension of the protrusion. This condition can be seen in an asymptomatic population, making the imputability with pain challenging.[31]

Disk Extrusion

Disk extrusion corresponds to a more extreme extension of the disk beyond the intervertebral margins, with the base against the disk of the origin narrower than the diameter of the extruding material itself (►**Fig. 1b**) or with no connection between the material and the disk of origin (sequestration). Contrary to disk protrusions, disks extrusions are usually symptomatic.[31]

Disk extrusion with sequestration is a focal disk displacement when extruded disk material has no continuity with the disk of origin.[3] Two variants exist:

- Subligamentous sequestration: Variant of an extrusion with sequestration that occurs when the nucleus pulposus material splays along the posterior longitudinal ligament. It appears spindle shaped on imaging.[32]
- Transligamentous sequestration: Disk material displacement results in full-thickness disruption of the annulus fibrosus fibers and posterior longitudinal ligament. A fragment may stay at the level of the disk or may migrate superiorly or inferiorly. Pain and neurologic symptoms may fluctuate with the migration of the free fragment within the spinal canal.[3,32]

Intravertebral Disk Herniations (Schmorl's Node)

Degenerative changes of end plates are very frequent and correspond to microbreaks with an irregularity aspect on imaging. A very large end-plate defect with a substantial volume of migrated nucleus pulposus material corresponds to an intravertebral disk herniation often called Schmorl's node (SN) (►**Fig. 4a, b**).

SN is fairly common and can be produced by any process that weakens either the cartilaginous plate covering the

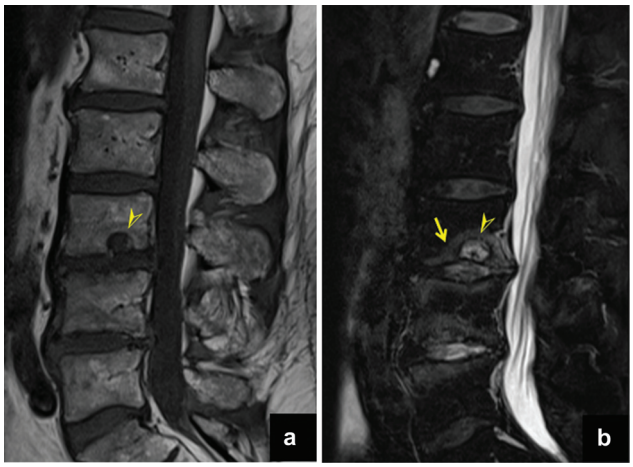

Fig. 4 A 50-year-old patient. (**a**) Sagittal T1-weighted magnetic resonance (MR) image. (**b**) Sagittal fat-saturated T2-weighted MR image: lumbar disk degenerative disease. Acute edematous intravertebral disk herniation (Schmorl's node) of the inferior end plate of L3 (arrowheads), with edema surrounding a preexisting intravertebral herniation (edema appearing as high signal on T2-weighted images) (arrow).

superior and inferior surfaces of the vertebral body or the subchondral trabeculae of the vertebra. SNs are often associated with Scheuermann's disease but are also seen in common DDD. SNs are always asymptomatic. However, the contact between SN and the bone marrow of the vertebra can lead to inflammation, responsible for back pain[33] (►**Fig. 4a, b**).

SNs can be detected on a radiograph, although they can be better analyzed with CT where a surrounding sclerosis is generally seen. MRI is the best examination to reveal an acute edematous SN. It shows blurred boundary edema surrounding a preexisting intravertebral herniation (edema appearing as high signal on T2w images and low signal on T1w images), a distinction that radiographs or CT cannot make. Edematous SN can also have an important fluorodeoxyglucose uptake on positron emission tomography that can lead to wrong diagnoses, especially in the oncology setting.[34]

Metabolic Conditions

Finally, some metabolic conditions can be responsible for the onset or accelerated DDD. Mucopolysaccharidoses (such as Morquio's syndrome) are a group of diseases characterized by the abnormal accumulation of glycosaminoglycans where the osteoarticular system is always involved, particularly the lumbar spine (DDD and vertebral malformations).

Diabetes mellitus modifies the composition of the intervertebral disk and causes accelerated DDD, sometimes leading to real destruction of the diskovertebral complex (Charcot's spine).[35]

Alkaptonuria is a rare genetic disease associated with the accumulation of homogentisic acid and its oxidized/polymerized products that leads to the deposition of melanin-like pigments (ochronosis) in connective tissues.[36] On imaging, ochronosis generally presents as a multilevel "vacuum phenomenon" with disk calcifications.

Active Disk Pain

Definition, Anatomy, and Biomechanics

Active disk pain is similar to disk pain, with the addition of inflammatory signs (pain and stiffness usually worsening in the morning and after inactivity, with effectiveness of anti-inflammatory drugs). This syndrome usually affects middle-age adults (< 55 years). The anatomical entity responsive for this symptomatology is active diskopathy.

MRI is the gold standard to reveal active diskopathy. The same signs of DDD can be seen with added vertebral end-plate subchondral bone changes. The affected levels are mostly L4–L5 and L5–S1.

Imaging

-On imaging, the vertebral end-plate subchondral bone changes adjacent to DDD are classified into three groups[37] (►**Fig. 5**):

- Modic 1 (vertebral end-plate subchondral bone edema)
- Modic 2 (vertebral end-plate subchondral fatty degeneration)
- Modic 3 (vertebral end-plate subchondral fibrotic or sclerotic changes)

Modic 1 changes are rarely observed in asymptomatic patients but are detected in up to 46% of patients with CLBP.[38] Modic 2 and 3 correspond to clinical and biological healing stages of the same dynamic process, associated with decreased inflammation-related symptoms.[5]

On MRI, Modic 1 signal changes are characterized by a low-intensity signal on T1w sequences and high signal on T2w sequences with enhancement on gadolinium chelate T1w sequences (bone marrow edema) (►**Fig. 5**). Modic 1 may also be associated with early sclerotic changes on CT. Both on CT and MRI, an erosive aspect with well-defined end plates is possible.

Modic 2 signal changes are characterized by a high signal both on T1w and T2w (bone marrow fatty degeneration).

Modic 3 signal changes are characterized by a low-intensity signal both on T1w and T2w sequences (bone marrow fibrosis/sclerosis). This stage is less frequent and associated with extensive bone condensation on radiographs/CT.[39]

All these Modic end-plate changes are often asymmetric with variable anteroposterior extension.

Modic 1 degenerative signal changes may mimic an infection or other inflammatory diskitis (Andersson lesion in spondyloarthropathy or calcium pyrophosphate dihydrate deposition diskitis).[40] However, some imaging signs make it possible to distinguish these entities from active DDD. Infection progresses very quickly, with osteolytic ill-defined end plates, and it is often associated with thickening or collections of the paravertebral soft tissues.[41] The edema of bone marrow for inflammatory diskitis (Andersson lesion or calcium pyrophosphate dehydrate diskitis) usually has well-demarcated boundaries with sclerosis on CT. Finally, the demonstration of other corners with bone marrow edema, fatty metaplasia, or erosions may suggest a spondyloarthropathy. The demonstration of calcific deposits may indicate a calcium pyrophosphate dihydrate disease.

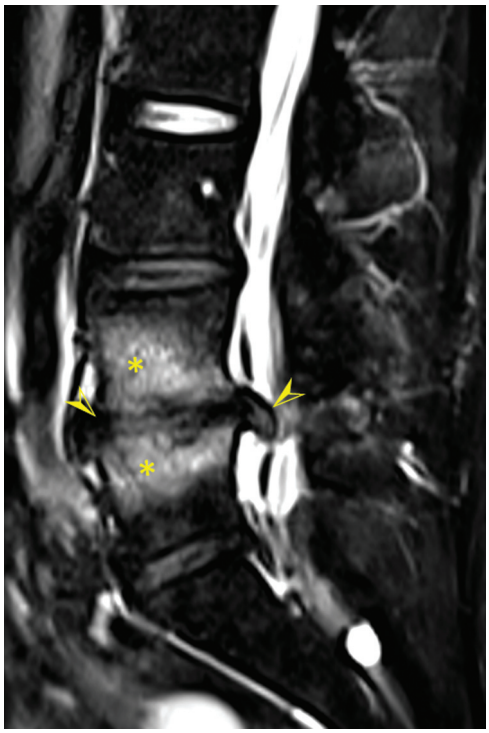

Fig. 5 A 38-year-old patient. Sagittal fat-saturated T2-weighted magnetic resonance image: L3–L4, L4–L5, and L5–S1 degenerative disk diseases. At the L4–L5 level, erosive pattern with irregular vertebral end plates and extensive subchondral bone edema (asterisk) corresponds to an active disk disease (Modic type 1). Note association with an L4–L5 disk anterior and posterior protrusion (arrowheads).

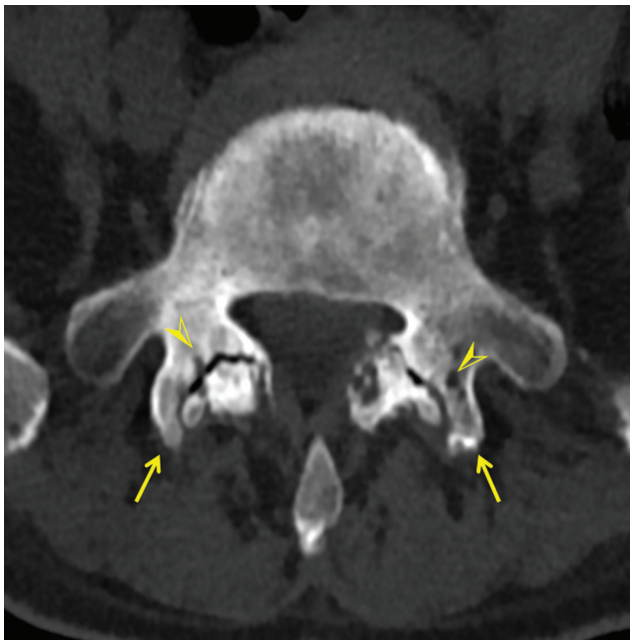

Fig. 6 An 80-year-old patient. Axial computed tomography image at the L5–S1 level: bilateral facet joint osteoarthritis. Degenerative changes include narrowing of the facet joint space, subarticular bone erosions (arrowheads), osteophyte formation, and hypertrophy of the articular process (arrows), corresponding to a grade 3 Pathria classification.

Facet Joint Osteoarthritis Pain

Definition, Anatomy, and Biomechanics

Facet joint osteoarthritis pain is characterized by paralumbar pain, worsening after prolonged walking or sitting, without the characteristics of disk pain. Also, the physical examination is normal. The anatomical entity responsive for this symptomatology is facet joint osteoarthritis (FJOA).

The lumbar facet joints form the posterolateral articulations connecting the vertebral arch of one vertebra to the arch of the adjacent vertebra. Contrary to the intervertebral disk, they are true synovial joints; each facet joint may contain between 1 and 1.5 mL of fluid. The basic anatomical unit of the spine, often referred to as the three-joint complex, consists of the pair of facet joints and the intervertebral disk.

Facet joints oriented parallel to the sagittal plane provide substantial resistance to axial rotation but minimal resistance to shearing forces (backward and forward sliding), whereas joints oriented more in a coronal plane tend to protect against flexion and shearing forces but provide minimal protection against rotation.[42] In young people, the facet joints are quite strong, capable of supporting almost twice their body weight. As aging occurs, the joints become weaker and more biplanar, transitioning from a largely coronal orientation to a more prominent sagittal positioning. Even though most of the axial load is borne by the intervertebral disks, the facet joints, as the two other components of the three-joint complex, also play a role in weight-bearing (typically 3–25% of the axial burden that can increase even higher in patients with DDD facet arthritis).[43] Even when associated with DDD, facet joint involvement is probably the nociceptive source incriminated in most of CLBP, potentially because its capsule is richly innervated.[44]

FJOA pain is common in the lumbar spine. Contrary to disk pain and active disk pain, it usually affects older adults (> 65 years). It is exacerbated by hyperlordosis, overweight, and disk degeneration that increase posterior mechanical spinal pressures. Nevertheless, the presence of FJOA is not always associated with pain. For instance, ~ 90% of asymptomatic young elite tennis players may present FJOA.[10]

Imaging

On imaging, the classic hallmarks of FJOA involve both degenerative and proliferative features: narrowing of the facet joint space, sagittal orientation modification, subarticular bone erosions, subchondral cysts, edema, osteophyte formation, hypertrophy of the articular process, and formation of synovial cysts (►**Fig. 6**).[45] Topographically, FJOA is not distributed evenly in the lumbar region. The classic radiographic features of FJOA are most common at the lower levels, L4–L5 followed by L5–S1.

CT and MRI are equally useful in demonstrating morphological changes in facet joints.[46] However, MRI is better able to reveal bone edema and synovial cysts but tends to underestimate the severity of FJOA compared with CT.[47]

The presence of subchondral bone edema may be a good marker of the facet joint origin of CLBP (present in ~ 40% of patients with back pain attributed to FJOA).[48]

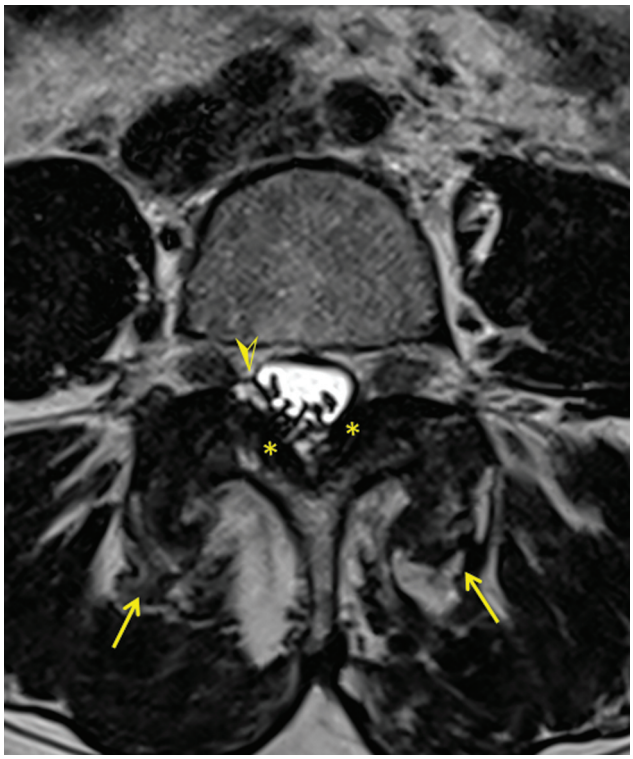

Fig. 7 A 65-year-old patient. Axial T2-weighted magnetic resonance image at the L3–L4 level: bilateral facet joint osteoarthritis with right synovial cyst responsible for a moderate foraminal stenosis (arrowhead). Bilateral ligamentum flavum hypertrophy (asterisks) and osteophyte formation with hypertrophy of the articular process (arrows), corresponding to a grade 3 Pathria classification.

Synovial facet joint cysts are usually high signal on T2w images. They can also have a high signal on T1w images if there is a hemorrhagic or proteinaceous component. The objective of imaging is to detect if they seem compressive on other structures, particularly on the path of nerve roots (►**Fig. 7**).

Pathria's classification is generally used for grading FJOA on CT (►**Fig. 6**):

- Grade 1: Facets with joint space narrowing
- Grade 2: Facets with narrowing and sclerosis or hypertrophy
- Grade 3: Facets with severe degenerative disease encompassing narrowing, sclerosis, and osteophytes

Due to the sagittal orientation modification of facet joints, FJOA can also be responsible for a degenerative spondylolisthesis. The motion-related abnormalities must be sought on standing position dynamic radiographs (flexion-extension) to assess instability. Indeed, MRI and CT imaging cannot correctly grade a degenerative spondylolisthesis.

Multifactorial Painful Syndromes

We include in the category of multifactorial painful syndromes lumbar spinal stenosis pain, foraminal stenosis pain, and instability pain, based on our experience/practice-based approach.

Lumbar Spinal Stenosis Pain

Definition, Anatomy, and Biomechanics

The specific symptom of spinal stenosis pain is neurogenic claudication causing numbness and weakness in the legs and a reduced ability to walk for an extended length of time. Leg pain due to added foraminal stenosis and facet joint osteoarthritis may accompany claudication. Back pain may or may not be present. Pain is usually relieved in lumbar kyphosis. The physical examination is normal.

The anatomical entity responsible for this symptomatology is lumbar spinal stenosis (LSS). The lumbar spinal canal consists of a central canal and on each side of the vertebra of a lateral canal followed by a neural foramen. The central canal contains the dural sac with the nerve roots, the epidural fat, and vascular elements. The lateral canal is a space in which the nerve root travels from the central canal to the neural foramen. It is subdivided from top to bottom into the disco-radicular pathway and the lateral recess. The lateral recess is always visible in L5 and S1, in $\sim$ 75% of the cases in L4, but it is exceptionally identifiable in the upper part of the lumbar canal. Thus the intracanal path of each root can be divided into four segments: the dural emergence (1); the disk segment (2), where the root is located in the disco-articular pathway between the disk and the facet joint; the pedicle segment (3) in the lateral recess; and the foraminal segment (4) in the neural foramen.

LSS is a pathologic condition resulting from a reduction in size of the lumbar spinal canal. It may be symptomatic, if adjacent neurovascular structures (particularly nerve roots) are compressed. The overall prevalence of LSS is $\sim$ 30% in the overall population and $\sim$ 50% in individuals $>$ 60 years of age.[49]

Imaging

On imaging, according to its anatomical location, LSS is classified as central, lateral, or combined stenosis. Both qualitative and quantitative approaches are possible.

Qualitative Approach

Preexisting constitutional LSS (usually resulting from congenitally shortened pedicles) can predispose to the syndrome. Constitutional stenosis is rarely compressive itself because of the constitutional development adjustment between the size of the canal and that of the dural sac and the epidural fat. However, the reduced thickness of the epidural fat and the reduced amount of cerebrospinal fluid (CSF) make the nerve roots more vulnerable to compression by a disk protrusion or osteophyte. The presence of constitutional LSS is therefore susceptible to decompensate when degenerative changes narrow the lumbar spinal canal.

CT and MRI are the best imaging techniques to identify the degenerative changes potentially responsible for LSS, associated or single:

- Bulging disk, herniation, or disk osteophyte complex (disk osteophyte bar)
- Posterior facet joints hypertrophy due to osteoarthritis

- Synovial facet cysts
- Hypertrophy of ligament flava that may also ossify
- Ossification of the posterior longitudinal ligament
- Epidural lipomatosis
- All pathologies likely to affect the bone and discoligamentous structures (Paget's disease, acromegaly, etc.)

Furthermore, lumbar instability (with degenerative or isthmic spondylolisthesis), defined as abnormal motion of the disco-vertebral complex due to physiologic stress, can also create or aggravate a preexisting compression (a condition called "dynamic stenosis"). It is also important to note that, in the particular case of lumbar scoliosis, compression can be found on the concave side of the deformity or in the presence of a rotational dislocation.

Even if MRI allows a good morphological analysis of the elements narrowing the spinal canal, osteophytes and ligament calcifications are less well analyzed than on CT.[50] The degree of stenosis can be based on morphological criteria: mass effect on the dural sac, shape of the dural sac, obliteration of the anterior CSF lamina, and relationship between the CSF and the cauda equina roots.[51,52]

Nevertheless, CT may fail to recognize or underestimate a degenerative spondylolisthesis because it is performed in the decubitus position.[53] Neither CT nor MRI accounts for the dynamic changes that may narrow the canal in the standing position. Radiographs may show spondylolisthesis and degenerative spinal changes (flexion-extension views can also be performed to verify vertebral instability). Apart from this situation, they are neither sensitive nor specific and do not allow an assessment of the impact on the dural sac.

Lumbar myelography is used to assess the dynamic nature of LSS (►**Fig. 8**). Because of its invasive nature, it should be performed in uncertain presurgical situations to clearly determine which levels should be operated. It allows the location and severity of segmental narrowing in a standing position. Lumbar myelography can be coupled to CT (CT myelography). This technique allows a precise morphological study of the structures compressing the dural sac and of the roots silhouetted by the contrast agent. Above the stenosis, the roots may take on a sinuous and wrinkled appearance.

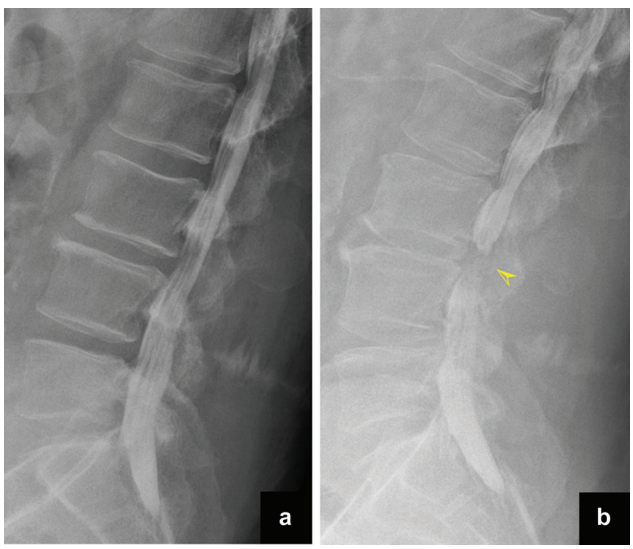

Fig. 8 A 70-year-old patient with L3–L4 dynamic stenosis at myelography. (**a**) In a sitting position, the contrast column is of a homogeneous caliber. (**b**) When standing, a L3–L4 spinal stenosis appears (arrowhead).

Even if MRI may overestimate stenosis, particularly because of cauda equina root clumping and/or CSF flow artifacts, the use of T2w three-dimensional (3D) sequences allows for a better analysis of the stenosis components and the degree of stenosis.[54] Thus MRI examination without gadolinium chelate injection and with T2w 3D sequences has replaced lumbar myelography and is now considered the best imaging modality for accessing LSS.[55]

The qualitative grading/morphological classification system (Schizas score) is often used to quantify lumbar stenosis.[56] The grading is based on the CSF-to-rootlet ratio as seen on axial T2w images and was conceived following observation of the different patterns according to which the rootlets were disposed within the dural sac while the patient rested supine during MR acquisition. These four grades are described[56]:

- Grade A (no or minor stenosis): CSF clearly visible inside the dural sac but with an inhomogeneous distribution.
- Grade B (moderate stenosis): The rootlets occupy the whole of the dural sac, but they can still be individualized. Some CSF is still present, giving a grainy appearance to the sac (►**Fig. 9a**).
- Grade C (severe stenosis): No rootlets can be recognized; the dural sac demonstrates a homogeneous gray signal with no CSF signal visible. Epidural fat is present posteriorly (►**Fig. 9b**).
- Grade D (extreme stenosis): In addition to no recognizable rootlets, there is no epidural fat posteriorly (►**Fig. 9c**).

Epidural lipomatosis is a relatively rare but well-known condition characterized by the overgrowth of epidural adipose tissue within the spinal canal.[57] It can cause symptoms that mimic LSS, even though the osseous diameters of the spinal canal are normal. The five main etiologies are exogenous steroid use, endogenous steroid hormonal disease, obesity, surgery-induced, and idiopathic.[57] Epidural lipomatosis is easily detected on CT and MRI. The epidural fatty hypertrophic component appears as high signal on T1w images. The dural sac typically displays a star-shaped appearance on axial MR slices or with undulating and concave margins (►**Fig. 10**).

Quantitative Approach

As mentioned earlier, LSS is defined as an abnormal narrowing of the central canal and/or lateral recesses.

Narrowing of the Central Canal

Radiologic diagnosis of LSS is complicated by a large number of imprecisely defined and inadequately evaluated methods of measurement.[58] On CT, a 10-mm cutoff value of the anteroposterior diameter of the osseous lumbar spinal canal

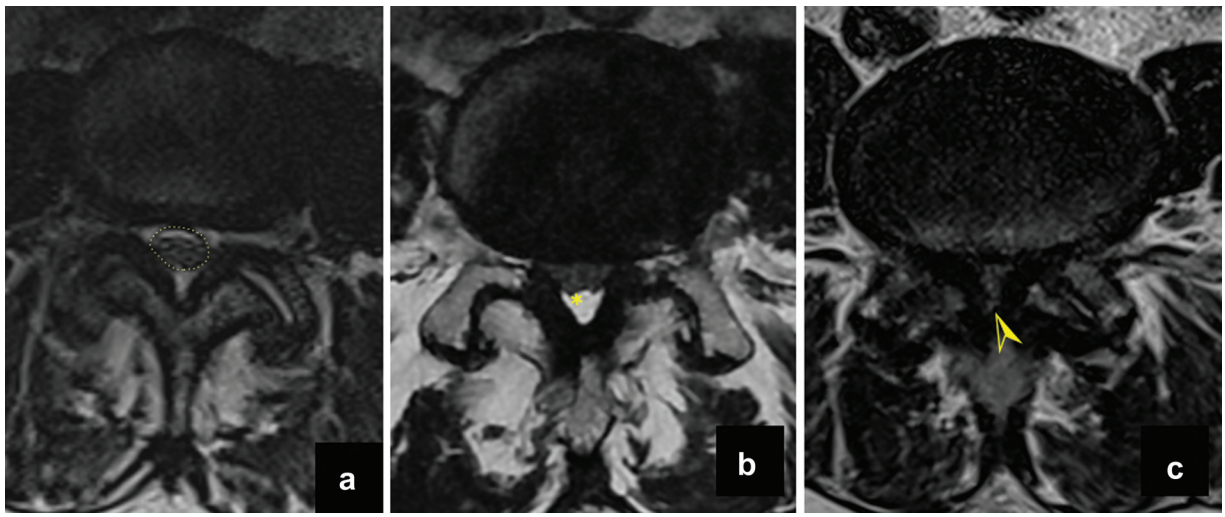

Fig. 9 Three different patients with axial T2-weighted magnetic resonance images to illustrate the qualitative grading classification system (Schizas score) to quantify lumbar stenosis. (**a**) Grade B (moderate stenosis): The rootlets occupy the whole of the dural sac, but they can still be individualized. Some cerebrospinal fluid (CSF) is still present, giving a grainy appearance to the sac. The dural sac is outlined by a dotted line that corresponds to the dural sac cross-sectional area. (**b**) Grade C (severe stenosis): No rootlets can be recognized; the dural sac demonstrates a homogeneous gray signal with no CSF signal visible. Epidural fat is present posteriorly (asterisk). (**c**) Grade D (extreme stenosis): In addition to no recognizable rootlets, there is no epidural fat posteriorly (arrowhead).

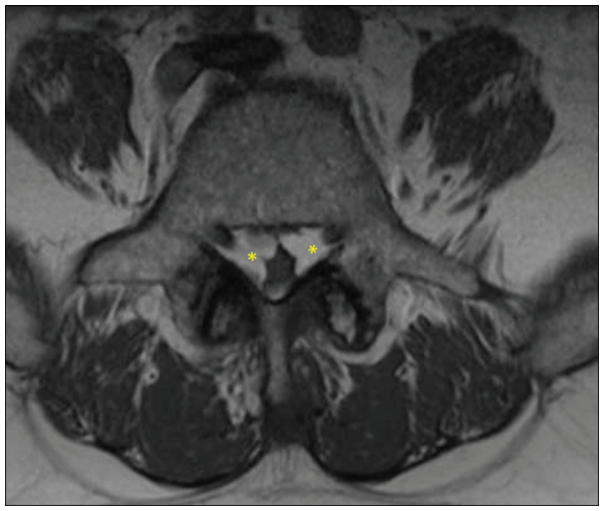

Fig. 10 A 52-year-old patient. Axial T1-weighted magnetic resonance image at the L5–S1 level: epidural lipomatosis. Epidural fatty hypertrophic component at L5–S1 image appears as high signal on T1-weighted images (asterisks), responsible for a stenosis of the dural sac with undulating margins.

is generally used for determining absolute LSS and a 12-mm cutoff value for relative stenosis.[59] The transverse diameter of the osseous spinal canal can also be measured but is of less interest, all the more because its value increases steadily from L1 to L5.[60]

All these measurements must be interpreted with caution because they do not account for body size, pedicle length, or interlaminar angle. MRI measurements of the canal are not as accurate as CT due to the low signal of the cortical bone, ligaments, and the lower spatial resolution.

LSS can also be identified by measuring the reduction of the surface area of the dural sac (dural sac cross-sectional area [DSCA]) on axial CT or MR images. Different methods of measurement and thresholds concerning this issue have been described in the literature.[61] Axial images angled vertically to the dural sac are required for this measurement. Thus T2w images, which provide a good contrast between the dural sac and the neighboring canal structures, are recommended (►**Fig. 9a**). The threshold of 100 mm^2 is an established and expressive value for the diagnosis of LSS.[58]

Measurement of DSCA and morphological grading (Schizas score) are good to excellent radiologic indicators differentiating patients with simple disk pain from those with LSS pain.[49] Indeed, stenosis grades C and D or DSCA inferior to 75 mm^2 are both linked to an increased risk of failure of conservative treatment and the need for surgery.[56]

Narrowing of the Lateral Recesses

As with stenosis of the central canal, acquired narrowness of the lateral recess may be secondary to the presence of a disk or osteophytic material anteriorly, an osteophyte from facet joint osteoarthritis posteriorly, or a degenerative spondylolisthesis, especially when the recess is constitutionally narrow ($<$ 3 mm of anteroposterior diameter on CT or MRI).

Foraminal Stenosis Pain

Definition and Anatomy

Foraminal stenosis pain is characterized by foraminal claudication, with pain relieved in lumbar kyphosis and intensified when sitting with the back straight.

After having passed the lateral recess, the nerve root reaches the neural foramen. The root emergence is located one level above its exit from the spinal canal through the neural foramen. The anatomical entity responsible for foraminal stenosis pain is often the association of DDD and FJOA.

Imaging

Qualitative Approach

From a qualitative point of view, imaging can reveal the cause of acquired foraminal stenosis:

- A narrowing of the intervertebral disk, responsible for the reduction of the height of the foramina of the same level (Crock's syndrome). The roots can then be compressed between the lower face of the pedicles and the tip of the upper articular processes of the underlying vertebra.
- Hypertrophic FJOA, mainly seen in hyperlordosis that spares the intervertebral disks but overloads the facet joints (sometimes with a facet joint cyst).
- Degenerative or isthmic spondylolisthesis.

On CT or MRI, neural foramina can be considered narrowed if the fat surrounding the nerve root is not visible anymore (►**Fig. 11**).

Quantitative Approach

From a quantitative point of view, the maximal anteroposterior diameter of the neural foramina can be assessed on sagittal MR or CT images. Measurement below the threshold of 3 mm indicates the presence of a foraminal stenosis.[61]

A grading system for foramen stenosis caused by DDD and FJOA can be used, based on the depiction of the foraminal components: nerve, vessels, and fat (►**Fig. 11**).[62]

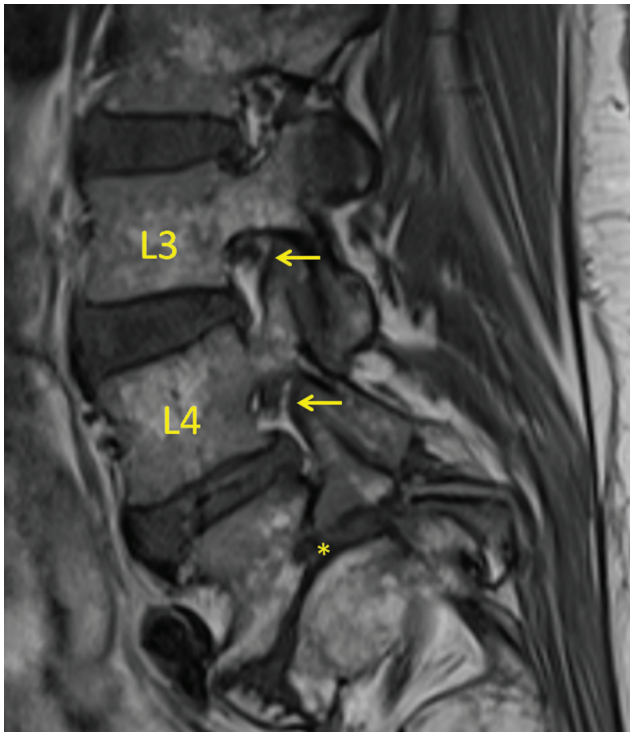

Fig. 11 A 61-year-old patient. Parasagittal T1-weighted magnetic resonance image showing foraminal stenoses. The L3–L4 and L4–L5 disk bulging is responsible (arrows) for a minimal foraminal stenosis (grade 1) and a moderate foraminal stenosis (grade 2), respectively. At the L5–S1 level, combination of a reduction of height of the L5–S1 disk and hypertrophic facet joint osteoarthritis is responsible (asterisk) for a severe foraminal stenosis (grade 3).

- – Grade 1: No stenosis or minimal stenosis
- – Grade 2: Stenosis without evidence of root compression
- – Grade 3: Stenosis with content of the foramen not well identified, signifying that the nerve root is compressed (caused by DDD, hypertrophic FJOA, or the ligamentum flavum)

Instability Pain

Biomechanically, spinal stability can be divided into vertical and horizontal instability[3]:

- Vertical instability is usually related to processes involving vertebral bodies: either due to focal conditions (for instance, a focal lytic lesion) or diffuse conditions (for instance, osteoporosis).
- Horizontal (intervertebral or segmental instability) is the instability due to the degeneration of the intervertebral disk, facet joints, and ligamentous structures.

Degenerative instability consists of a pure motion dysfunctional syndrome with two possibilities:

- Microinstability, where there is no or minimal anatomical changes, undetectable on imaging
- Overt instability that can be detected radiologically[3]

We next discuss spondylolisthesis and spinal segment deformity, respectively. For these two conditions, the diagnosis of intervertebral instability is based on both the direct and indirect radiologic findings of abnormal vertebral motion.

Spondylolisthesis

Spondylolisthesis is a condition in which a vertebra slips forward over the vertebra below. The vertebra can slip anteriorly (anterolisthesis), posteriorly (retrolisthesis), or on each lateral edge of the vertebra (laterolisthesis). Laterolisthesis is discussed in the section on spinal segment deformity.

Anterolisthesis

The two main types of anterolisthesis (degenerative and isthmic) are a common cause of low back pain and radiculalgia, both relieved by lumbar kyphosis. Degenerative spondylolisthesis corresponds to the instability of one or more vertebral segments due to lumbar spine degenerative changes. It generally occurs at the three lower lumbar levels (L3–L4, L4–L5, and L5–S1) and is often responsible for LSS.

Both the anterior part (intervertebral disk) and the posterior part of the spine (facet joints) may be responsible for this type of instability. However, FJOA plays a central role in this type of pathology. FJOA is frequently erosive, with an abnormally sagittal joint space that favors vertebral slippage. Thus this condition is most common among older adults, particularly women. Degenerative anterolisthesis is usually moderate (< 1 cm), especially compared with isthmic lysis. The clinical symptoms, however, are often more marked. Degenerative anterolisthesis is one of the main causes of LSS, contrary to isthmic lysis where there is no

narrowing of the central canal due to the rupture of the posterior arch.

Direct Signs

CT and MRI are problematic for demonstrating direct signs of anterolisthesis. In fact, this condition can "self-reduce" without the normal axial load of the standing position. That is why dynamic radiographs are useful to detect an anterolisthesis and to grade it. A flexion-extension bending view is usually performed as a functional way to access spinal instability. An oblique view can be added to visualize the pars interarticularis if an isthmic anterolisthesis is suspected.[27] On flexion-extension radiographs, values of 10 degrees for sagittal rotation and 4 mm for sagittal translation are usually used to infer instability.[63] Thus degenerative anterolisthesis can be divided into a dynamic subtype (instability on flexion/extension radiographs) and a static subtype (no radiologic evidence of instability).

Meyerding's classification is often used to grade anterolisthesis. It is based on the ratio of the overhanging part of the superior vertebral body to the anteroposterior length of the adjacent inferior vertebral body (►**Figs. 12** and **13**):

- Grade 1: 0 to 25%
- Grade 2: 25 to 50%
- Grade 3: 50 to 75%
- Grade 4: 75 to 100%
- Grade 5: > 100% (spondyloptosis)

This classification is useful for isthmic anterolisthesis but not for degenerative ones (always grade 1).

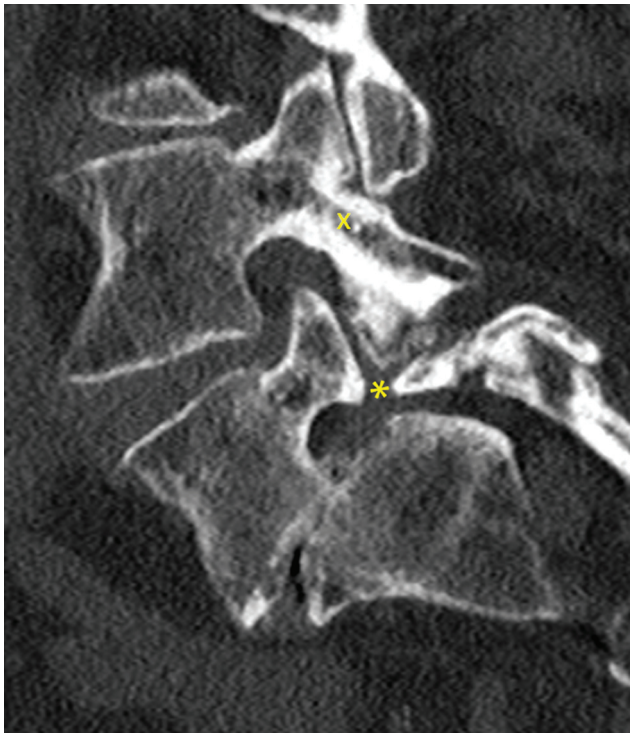

Fig. 12 A 45-year-old patient. Isthmic anterolisthesis of L5 grade 2 of Meyerding's classification with marked degenerative L5–S1 disk disease. Note L5 isthmic rupture (asterisk) and L4 normal isthmus (cross).

On CT, axial slices show loss of alignment of the facet joint surfaces with disruption of the articulo-laminar arch and anterior uncovering of the inferior articular process of the overlying vertebra that projects into the spinal canal. This anterior protrusion is responsible for the narrowing of lateral recesses. These abnormalities may be bilateral and symmetrical, asymmetric, or unilateral.

Sagittalization and straightness of the facet joint space are usually present. On sagittal reformatted images, it is possible to assess the compression of the dural sac between the posterior arch of the slipping vertebra and the posterosuperior corner of the body of the underlying vertebra (especially in the case of bilateral and symmetrical subluxation), and that of the foramina by the adjoining osteophytosis. It should be noted that asymmetric subluxation of the facet joints favors rotational shearing of the disk, sometimes with foraminal extrusion on the side of the rotational slip.

MRI provides the same information (►**Fig. 13**), although the analysis of degenerative facet lesions is less detailed than on CT. Nevertheless, T2w sequences provide information on the state of hydration of the intervertebral disks, edema of facet joints, and/or interspinous bursitis.

Sacco-radiculography (detailed in the section about LSS) is now rarely performed preoperatively but is worthwhile to look for an increase of a stenosis between a sitting and standing position, in flexion and in extension, but also to

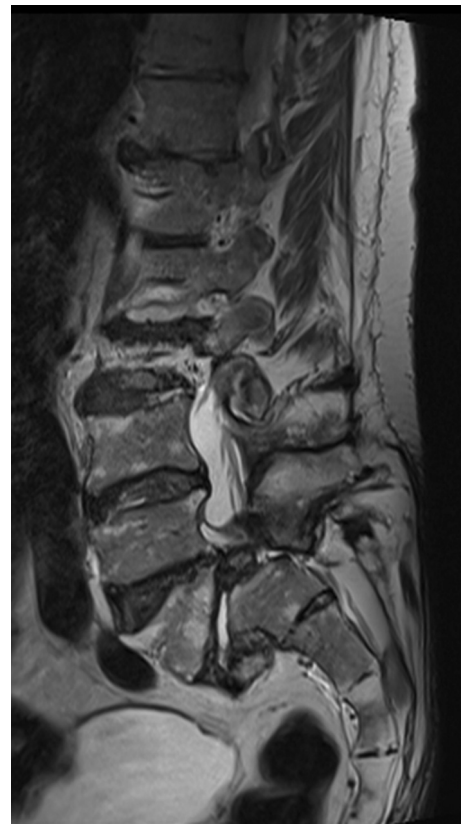

Fig. 13 An 80-year-old patient. L5–S1 Isthmic anterolisthesis grade 4 of Meyerding's classification, so significant that it is even responsible for an L5–S1 spinal stenosis (which is rare in isthmic spondylolisthesis) with a dysplastic aspect of the L5 vertebra. A vertebral osteoporotic fracture of L2 is also visible.

search for other spondylolisthesis above that would modify the number of levels treated in case of surgical management.

Indirect Signs

These are the indirect signs of instability that must be looked for on CT or MRI (described individually in the other sections of this article):

- Annular and nucleus pulposus fissures, in particular an intradiskal so-called vacuum phenomenon
- Traction enthesophytes
- Ligamentum flavum hypertrophy
- Facet joint cysts, intra-articular fluid, or edema of the wedges
- Lumbar interspinous bursitis

Lumbar interspinous bursitis (also called Baastrup's disease) is caused by contact between the posterior aspects of the spinous processes of the lumbar spine as a result of degenerative changes (►**Fig. 14**). It most commonly occurs in older adults with an incidence of ~ 80% among patients > 80 years of age, most and commonly visible at the L3–L4 and L4–L5 levels.[64] Pain is often exacerbated by spinal extension and relieved in flexion, such as in the fetal position.

It leads to the enlargement, flattening, and reactive sclerosis of apposed interspinous surfaces on radiographs or scan.[65] MRI is the best examination to reveal the bursitis that appears as high signal on T2w sequences (►**Fig. 14**).

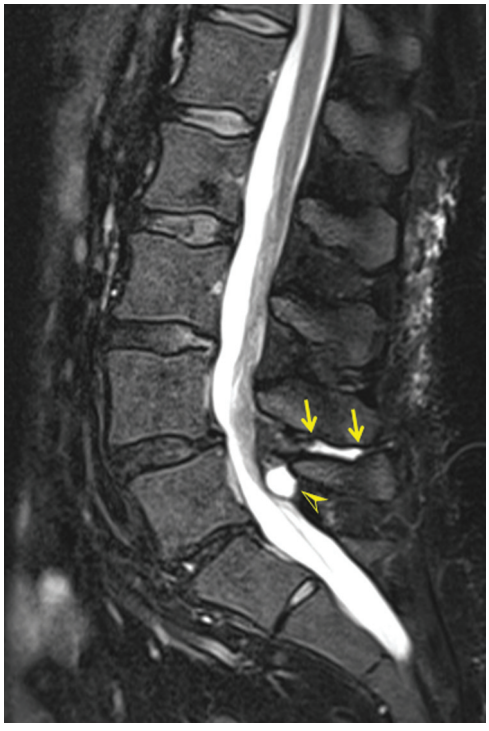

Fig. 14 A 47-year-old patient. Sagittal fat-saturated T2-weighted magnetic resonance image: degenerative disk disease at the L4–L5 and L5–S1 levels. Lumbar L4–L5 interspinous bursitis (Baastrup's disease) (arrows). Note the presence of an adjacent facet joint synovial cyst (arrowhead) and anterolisthesis of L4.

Retrolisthesis

Retrolisthesis corresponds to a posterior slippage of the vertebra. This condition is always degenerative and mainly located on at L1–L2 and L2–L3.

Radiographs show generally modest posterior vertebral slippage (average of 3 mm) generally associated with DDD. On sagittal reformatted images, CT and MRI allow analysis of the usually moderate impact of retrolisthesis on the central canal (►**Fig. 3**) and the often severe narrowing of the foramina.

Spinal Segment Deformity

Laterolisthesis corresponds to the lateral slippage of a vertebra over the vertebra below (also called "dislocation"). This condition is mainly observed after age 50 years.

Open dislocations (opening of the disk on the sliding side) are favored by ligament lesions, contrary to closed dislocations (narrowing of the disk on the sliding side) that are favored by FJOA. They are sometimes associated with significant rotational slippage (scoliotic deformation).

In degenerative scoliosis, a cycle of asymmetric deformity, asymmetric loading, and asymmetric degeneration occurs, with progressive scoliotic deformity leading to still further increased force transmission through the facet joint on the concave side of the curve.[45]

Radiographs show the disruption of the lateral angles of the vertebrae and assess the type of dislocation (open or closed) and the vertebral rotation. In idiopathic scoliosis, the measure of the Cobb angle is usual to follow degenerative scoliosis. Associated degenerative lesions can also be seen.

CT and MRI visualize the slippage and degree of vertebral rotation, the intracanal slippage of the facet joints, the central canal stenosis, and the degenerative disk and ligamentous changes that are often asymmetric.

MRI can reveal edema of the end plates localized at the scoliosis concavity that must not be confused with Modic changes (different from active DDD) (►**Fig. 15**).

Sacco-radiculography can confirm the intervertebral mobility associated with lateral and rotational intervertebral slippage.

Muscular Syndromes

Postural Syndrome

The pain usually occurs at the end of the day after sitting/standing for a long time. In postural syndrome, there is no significant damage or trauma to tissue.

Full-spine imaging, such as EOS (EOS Imaging, Paris, France), is useful to evaluate spinopelvic alignment. EOS is a very low-dose X-ray system with simultaneous acquisition of upright frontal and sagittal full-spine views avoiding vertical parallax distortion.[66] Among all the mechanisms that ensure the status of the spine, the muscles certainly play an underestimated role, particularly to correct a sagittal instability. Thus EOS may facilitate following the evolution of sagittal balance over time and could be interesting to detect and monitor these postural syndromes.[67]

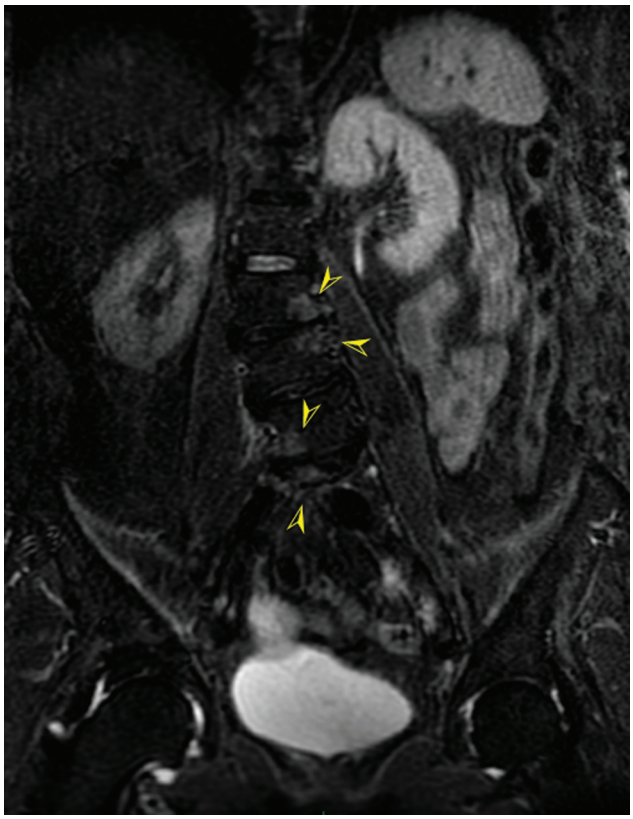

Fig. 15 A 73-year-old patient. Coronal fat-saturated T2-weighted magnetic resonance image: edema of the end plates localized at the scoliosis concavity not to be confused with Modic changes (different from active degenerative disk disease) (arrowheads).

In CT or MRI studies dealing with muscle diseases, the muscle cross-sectional area is a common measurement, even if to our knowledge no pathologic features have been described in postural syndromes.[68] Nevertheless, this measure seems to vary depending on the posture of the patient (upright, seated, or supine), which puts its usefulness in this positional pathologic context into perspective.[69]

An Example of Muscle Disease: Camptocormia

Camptocormia is a good example of a muscular condition responsible for back pain in older adults. It is an involuntary flexion of the thoracolumbar spine when standing, walking, or sitting that disappears completely in the supine position. Camptocormia occurs in association with primary and secondary myopathies, inflammation, dystonia, as a pharmacologic side effect, or as a functional disorder.[70] Primary muscle diseases with involvement of axial muscles, focal myositis, and secondary myopathies associated with neurodegenerative diseases seem to be the most frequent causes of camptocormia.

Muscle MRI is an important diagnostic tool in camptocormia because it shows typical muscle abnormalities and the extent of the muscle involvement (►**Fig. 16**). It generally involves the paravertebral, quadratus lumborum, and psoas muscles. In addition, imaging is necessary to exclude orthopaedic diseases. Acute changes in the muscle can be identified on short tau inversion recovery (STIR) sequences

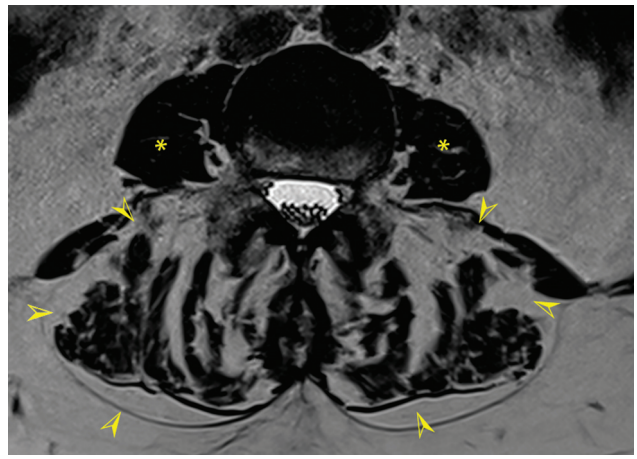

Fig. 16 A 50-year-old patient. Axial T2-weighted magnetic resonance image: fatty involvement of the paravertebral muscles (arrowheads) compared with psoas muscles that are preserved (asterisks).

(sensitive to intramuscular edema) or earlier using contrast-enhanced MR sequences.

However, muscle MRI has a lack of specificity. In particular, if muscle MRI shows exclusively acute changes, a muscle biopsy is indicated because STIR hyperintensities cannot prove myositis (pathologic STIR findings can also be seen in trauma, denervation, and a wide range of muscle diseases). Muscle MRI can be used to determine the most appropriate biopsy site.

The chronic changes of camptocormia must be analyzed on T1w sequences. These sequences can look for muscular atrophy, often asymmetric, and fatty degeneration shown by a high-intensity signal.

Conclusion

The knowledge of imaging patterns of lumbar degenerative spine disease allows the consideration of correlations with the clinical symptomatology. The goal is to identify the nociceptive source to better target and treat these extremely frequent and disabling pathologies.

Conflict of Interest
None declared.

References

1 Vos T, Flaxman AD, Naghavi M, et al. Years lived with disability (YLDs) for 1160 sequelae of 289 diseases and injuries 1990-2010: a systematic analysis for the Global Burden of Disease Study 2010. Lancet 2012;380(9859):2163–2196
2 Meucci RD, Fassa AG, Faria NMX. Prevalence of chronic low back pain: systematic review. Rev Saude Publica 2015;49(00):S0034-89102015000100408
3 Kushchayev SV, Glushko T, Jarraya M, et al. ABCs of the degenerative spine. Insights Imaging 2018;9(02):253–274
4 Gallucci M, Limbucci N, Paonessa A, Splendiani A. Degenerative disease of the spine. Neuroimaging Clin N Am 2007;17(01): 87–103
5 Nguyen C, Poiraudeau S, Rannou F. From Modic 1 vertebral-endplate subchondral bone signal changes detected by MRI to

the concept of 'active discopathy.'. Ann Rheum Dis 2015;74(08): 1488–1494
6 Nguyen C, De Sèze M, Rannou F. The challenges of precision medicine in chronic low back pain: lessons learned from active discopathy. Ann Phys Rehabil Med 2021;64(02):101504
7 Lotz JC, Haughton V, Boden SD, et al. New treatments and imaging strategies in degenerative disease of the intervertebral disks. Radiology 2012;264(01):6–19
8 Daly C, Ghosh P, Jenkin G, Oehme D, Goldschlager T. A review of animal models of intervertebral disc degeneration: pathophysiology, regeneration, and translation to the clinic. BioMed Res Int 2016;2016:5952165
9 Wocial KA, Feldman B, Mruk B, Sklinda K, Walecki J, Waśko M. Imaging features of the aging spine. Pol J Radiol 2021;86(01): e380–e386
10 Brinjikji W, Luetmer PH, Comstock B, et al. Systematic literature review of imaging features of spinal degeneration in asymptomatic populations. AJNR Am J Neuroradiol 2015;36(04):811–816
11 Adams A, Roche O, Mazumder A, Davagnanam I, Mankad K. Imaging of degenerative lumbar intervertebral discs; linking anatomy, pathology and imaging. Postgrad Med J 2014;90 (1067):511–519
12 Manchikanti L, Glaser SE, Wolfer L, Derby R, Cohen SP. Systematic review of lumbar discography as a diagnostic test for chronic low back pain. Pain Physician 2009;12(03):541–559
13 Rajeswaran G, Turner M, Gissane C, Healy JC. MRI findings in the lumbar spines of asymptomatic elite junior tennis players. Skeletal Radiol 2014;43(07):925–932
14 Yang S, Lassalle L, Mekki A, et al. Can T2-weighted Dixon fat-only images replace T1-weighted images in degenerative disc disease with Modic changes on lumbar spine MRI? Eur Radiol 2021;31 (12):9380–9389
15 Sollmann N, Mönch S, Riederer I, Zimmer C, Baum T, Kirschke JS. Imaging of the degenerative spine using a sagittal T2-weighted Dixon turbo spin-echo sequence. Eur J Radiol 2020;131:109204
16 Pfirrmann CWA, Metzdorf A, Elfering A, Hodler J, Boos N. Effect of aging and degeneration on disc volume and shape: a quantitative study in asymptomatic volunteers. J Orthop Res 2006;24(05): 1086–1094
17 Pfirrmann CWA, Metzdorf A, Zanetti M, Hodler J, Boos N. Magnetic resonance classification of lumbar intervertebral disc degeneration. Spine 2001;26(17):1873–1878
18 Ji Y, Hong W, Liu M, Liang Y, Deng Y, Ma L. Intervertebral disc degeneration associated with vertebral marrow fat, assessed using quantitative magnetic resonance imaging. Skeletal Radiol 2020;49(11):1753–1763
19 Raudner M, Schreiner MM, Weber M, et al. Compositional magnetic resonance imaging in the evaluation of the intervertebral disc: axial vs sagittal T_2 mapping. J Orthop Res 2020;38(09): 2057–2064
20 Thompson RE, Pearcy MJ, Downing KJW, Manthey BA, Parkinson IH, Fazzalari NL. Disc lesions and the mechanics of the intervertebral joint complex. Spine 2000;25(23):3026–3035
21 Tavakoli J, Elliott DM, Costi JJ. Structure and mechanical function of the inter-lamellar matrix of the annulus fibrosus in the disc. J Orthop Res 2016;34(08):1307–1315
22 Mulholland RC. The myth of lumbar instability: the importance of abnormal loading as a cause of low back pain. Eur Spine J 2008;17 (05):619–625
23 Shan Z, Chen H, Liu J, Ren H, Zhang X, Zhao F. Does the high-intensity zone (HIZ) of lumbar intervertebral discs always represent an annular fissure? Eur Radiol 2017;27(03):1267–1276
24 Wang ZX, Hu YG. Imaging analysis of the high-intensity zone on lumbar spine magnetic resonance images: classification, features and correlation with low back pain. J Pain Res 2021; 14:2981–2989
25 Izzo R, Guarnieri G, Guglielmi G, Muto M. Biomechanics of the spine. Part I: spinal stability. Eur J Radiol 2013;82(01):118–126
26 Heuck A, Glaser C. Basic aspects in MR imaging of degenerative lumbar disk disease. Semin Musculoskelet Radiol 2014;18(03): 228–239
27 Feydy A, Pluot E, Guerini H, Drapé JL. Osteoarthritis of the wrist and hand, and spine. Radiol Clin North Am 2009;47(04):723–759
28 Carragee EJ, Lincoln T, Parmar VS, Alamin T. A gold standard evaluation of the "discogenic pain" diagnosis as determined by provocative discography. Spine 2006;31(18):2115–2123
29 Thompson KJ, Dagher AP, Eckel TS, Clark M, Reinig JW. Modic changes on MR images as studied with provocative diskography: clinical relevance–a retrospective study of 2457 disks. Radiology 2009;250(03):849–855
30 Carragee EJ, Barcohana B, Alamin T, van den Haak E. Prospective controlled study of the development of lower back pain in previously asymptomatic subjects undergoing experimental discography. Spine 2004;29(10):1112–1117
31 Jensen MC, Brant-Zawadzki MN, Obuchowski N, Modic MT, Malkasian D, Ross JS. Magnetic resonance imaging of the lumbar spine in people without back pain. N Engl J Med 1994;331(02): 69–73
32 Fardon DF, Williams AL, Dohring EJ, Murtagh FR, Gabriel Rothman SL, Sze GK. Lumbar disc nomenclature: version 2.0: Recommendations of the combined task forces of the North American Spine Society, the American Society of Spine Radiology and the American Society of Neuroradiology. Spine J 2014;14(11):2525–2545
33 Kyere KA, Than KD, Wang AC, et al. Schmorl's nodes. Eur Spine J 2012;21(11):2115–2121
34 Zheng S, Dong Y, Miao Y, et al. Differentiation of osteolytic metastases and Schmorl's nodes in cancer patients using dual-energy CT: advantage of spectral CT imaging. Eur J Radiol 2014;83 (07):1216–1221
35 Boudabbous S, Paulin EN, Delattre BMA, Hamard M, Vargas MI. Spinal disorders mimicking infection. Insights Imaging 2021;12(01):176
36 Braconi D, Bernardini G, Bianchini C, et al. Biochemical and proteomic characterization of alkaptonuric chondrocytes. J Cell Physiol 2012;227(09):3333–3343
37 Böker SM, Bender YY, Adams LC, et al. Evaluation of sclerosis in Modic changes of the spine using susceptibility-weighted magnetic resonance imaging. Eur J Radiol 2017;88:148–154
38 Kjaer P, Korsholm L, Bendix T, Sorensen JS, Leboeuf-Yde C. Modic changes and their associations with clinical findings. Eur Spine J 2006;15(09):1312–1319
39 Nguyen C, Boutron I, Baron G, et al. Intradiscal glucocorticoid injection for patients with chronic low back pain associated with active discopathy: a randomized trial. Ann Intern Med 2017;166 (08):547–556
40 Singla A, Ryan A, Bennett DL, et al. Non-infectious thoracic discitis: a diagnostic and management dilemma. A report of two cases with review of the literature. Clin Neurol Neurosurg 2020;190:105648
41 Sans N, Faruch M, Lapègue F, Ponsot A, Chiavassa H, Railhac JJ. Infections of the spinal column—spondylodiscitis. Diagn Interv Imaging 2012;93(06):520–529
42 Cohen SP, Raja SN. Pathogenesis, diagnosis, and treatment of lumbar zygapophysial (facet) joint pain. Anesthesiology 2007; 106(03):591–614
43 Murtagh FR, Paulsen RD, Rechtine GR. The role and incidence of facet tropism in lumbar spine degenerative disc disease. J Spinal Disord 1991;4(01):86–89
44 Revel M, Poiraudeau S, Auleley GR, et al. Capacity of the clinical picture to characterize low back pain relieved by facet joint anesthesia. Proposed criteria to identify patients with painful facet joints. Spine 1998;23(18):1972–1976; discussion 1977
45 Gellhorn AC, Katz JN, Suri P. Osteoarthritis of the spine: the facet joints. Nat Rev Rheumatol 2013;9(04):216–224
46 Perolat R, Kastler A, Nicot B, et al. Facet joint syndrome: from diagnosis to interventional management. Insights Imaging 2018; 9(05):773–789

47 Modic MT, Steinberg PM, Ross JS, Masaryk TJ, Carter JR. Degenerative disk disease: assessment of changes in vertebral body marrow with MR imaging. Radiology 1988;166(1 Pt 1):193–199
48 Lakadamyali H, Tarhan NC, Ergun T, Cakir B, Agildere AM. STIR sequence for depiction of degenerative changes in posterior stabilizing elements in patients with lower back pain. AJR Am J Roentgenol 2008;191(04):973–979
49 Jain N, Acharya S, Adsul NM, et al. Lumbar canal stenosis: a prospective clinicoradiologic analysis. J Neurol Surg A Cent Eur Neurosurg 2020;81(05):387–391
50 Merlino J, Perisa J. Low back pain in a competitive cricket athlete. Int J Sports Phys Ther 2012;7(01):101–108
51 Lee GY, Lee JW, Choi HS, Oh KJ, Kang HS. A new grading system of lumbar central canal stenosis on MRI: an easy and reliable method. Skeletal Radiol 2011;40(08):1033–1039
52 Lehnen NC, Haase R, Faber J, et al. Detection of degenerative changes on MR images of the lumbar spine with a convolutional neural network: a feasibility study. Diagnostics (Basel) 2021;11 (05):902
53 Siebert E, Prüss H, Klingebiel R, Failli V, Einhäupl KM, Schwab JM. Lumbar spinal stenosis: syndrome, diagnostics and treatment. Nat Rev Neurol 2009;5(07):392–403
54 Macedo LG, Bodnar A, Battié MC. A comparison of two methods to evaluate a narrow spinal canal: routine magnetic resonance imaging versus three-dimensional reconstruction. Spine J 2016; 16(07):884–888
55 Rao D, Scuderi G, Scuderi C, Grewal R, Sandhu SJ. The use of imaging in management of patients with low back pain. J Clin Imaging Sci 2018;8:30
56 Schizas C, Theumann N, Burn A, et al. Qualitative grading of severity of lumbar spinal stenosis based on the morphology of the dural sac on magnetic resonance images. Spine 2010;35(21): 1919–1924
57 Kim K, Mendelis J, Cho W. Spinal epidural lipomatosis: a review of pathogenesis, characteristics, clinical presentation, and management. Global Spine J 2019;9(06):658–665
58 Waldt S, Gersing A, Brügel M. Measurements and classifications in spine imaging. Semin Musculoskelet Radiol 2014;18(03): 219–227
59 Andreisek G, Hodler J, Steurer J. Uncertainties in the diagnosis of lumbar spinal stenosis. Radiology 2011;261(03):681–684
60 Amonoo-Kuofi HS, Patel PJ, Fatani JA. Transverse diameter of the lumbar spinal canal in normal adult Saudis. Acta Anat (Basel) 1990;137(02):124–128
61 Mamisch N, Brumann M, Hodler J, Held U, Brunner F, Steurer JLumbar Spinal Stenosis Outcome Study Working Group Zurich. Radiologic criteria for the diagnosis of spinal stenosis: results of a Delphi survey. Radiology 2012;264(01):174–179
62 Splendiani A, Ferrari F, Barile A, Masciocchi C, Gallucci M. Occult neural foraminal stenosis caused by association between disc degeneration and facet joint osteoarthritis: demonstration with dedicated upright MRI system. Radiol Med (Torino) 2014;119 (03):164–174
63 Leone A, Guglielmi G, Cassar-Pullicino VN, Bonomo L. Lumbar intervertebral instability: a review. Radiology 2007;245(01): 62–77
64 Kwong Y, Rao N, Latief K. MDCT findings in Baastrup disease: disease or normal feature of the aging spine? AJR Am J Roentgenol 2011;196(05):1156–1159
65 Alonso F, Bryant E, Iwanaga J, Chapman JR, Oskouian RJ, Tubbs RS. Baastrup's disease: a comprehensive review of the extant literature. World Neurosurg 2017;101:331–334
66 Fechtenbaum J, Etcheto A, Kolta S, Feydy A, Roux C, Briot K. Sagittal balance of the spine in patients with osteoporotic vertebral fractures. Osteoporos Int 2016;27(02):559–567
67 Hasegawa K, Okamoto M, Hatsushikano S, et al. Standing sagittal alignment of the whole axial skeleton with reference to the gravity line in humans. J Anat 2017;230(05):619–630
68 Grimm A, Nickel MD, Chaudry O, et al. Feasibility of Dixon magnetic resonance imaging to quantify effects of physical training on muscle composition—a pilot study in young and healthy men. Eur J Radiol 2019;114:160–166
69 Shaikh N, Zhang H, Brown SHM, et al. The effect of posture on lumbar muscle morphometry from upright MRI. Eur Spine J 2020; 29(09):2306–2318
70 Margraf NG, Wrede A, Deuschl G, Schulz-Schaeffer WJ. Pathophysiological concepts and treatment of camptocormia. J Parkinsons Dis 2016;6(03):485–501